

# INTRODUCTION TO FREQUENCY MAP ANALYSIS

JACQUES LASKAR

*CNRS–Astronomie et Systèmes Dynamiques, Bureau des Longitudes  
3 rue Mazarine, 75006 Paris, France*

**Abstract.** Frequency map analysis is a numerical method which provides a clear representation of the global dynamics of many multi-dimensional systems, and which is particularly useful for systems of 3 degrees of freedom and more. The frequency map dependence with time also allows refined estimates of the diffusion of the orbits in the frequency domain. Here are presented some applications of frequency map analysis to the special case of a quasi-periodic perturbation, and to the study of the global dynamics of a 4 dimensional symplectic mapping with definite or indefinite torsion. The convergence of the frequency analysis algorithm on KAM solutions is demonstrated, and the asymptotic value of the error is provided.

## 1. Introduction

According to KAM theorem [11, 1, 22], in the phase space of a sufficiently close to integrable conservative system, many invariant tori will persist. Trajectories starting on one of these tori remain on it thereafter, executing quasiperiodic motion with fixed frequency vector depending only on the torus. The family of tori is parameterized over a Cantor set of frequency vectors, while in the gaps of the Cantor set chaotic behavior can—and generically does—occur. These slightly deformed tori are fixed structures of the system. It is possible numerically to find them, to straighten them out, and to interpolate between them to form an action-angle coordinate system in which regular (quasiperiodic) motion appears uniformly circular, and weakly chaotic motion stands out as a slight departure.

The search for approximate action-angle variables has been a constant preoccupation in celestial mechanics, since the early works of Laplace and Lagrange who were looking for mean elements in the planetary motions. It was then more formally stated through the works of Jacobi, Hamilton, and Poincaré [25] who set up the modern formulation for perturbation methods. In more recent years, besides theoretical stability results [6] inspired by the work of Nekhoroshev [23], the determination of approximate actions has been performed in the computation of the so-called “proper elements” of the minor planets [10]), in galactic dynamics [19], and in particle accelerator dynamics [28].

The frequency analysis method [4, 13, 14, 16, 17, 18] also relies on a fixed feature of the model system, but one which is simpler to compute; namely, the frequency vectors associated to each of the invariant tori. Although the frequencies are strictly speaking only defined and fixed on these tori, the frequency analysis algorithm will numerically compute

over a finite time span a frequency vector for any initial condition. On the KAM tori, this frequency vector will be a very accurate approximation of the actual frequencies, while in the chaotic regions, it will provide a natural interpolation between these fixed frequencies.

## 2. Frequency maps

Let us consider a Hamiltonian system with  $n$  degrees of freedom close to integrable in the form

$$H(I, \theta) = H_0(I) + \varepsilon H_1(I, \theta), \quad (1)$$

where  $H$  is real analytic for  $(I, \theta) = (I_1, \dots, I_n, \theta_1, \dots, \theta_n) \in B^n \times \mathbb{T}^n$ , where  $B^n$  is a domain of  $\mathbb{R}^n$  and  $\mathbb{T}^n$  is the usual  $n$ -dimensional torus.

For  $\varepsilon = 0$ , the Hamiltonian reduces to  $H_0(I)$  and is integrable. The equations of motion are then for all  $j = 1, \dots, n$

$$\dot{I}_j = 0, \quad \dot{\theta}_j = \frac{\partial H_0(I)}{\partial I_j} = \nu_j(I), \quad (2)$$

which gives in the complex variables  $z_j = I_j \exp i \theta_j$ ,

$$z_j(t) = z_{j0} e^{i \nu_j t}, \quad (3)$$

where  $z_{j0} = z_j(0)$ . The motion in phase space takes place on tori, products of true circles with constant radii  $I_j = |z_j(0)|$ , which are described at constant velocity  $\nu_j(I)$ . If the system is nondegenerate, that is if

$$\det \left( \frac{\partial \nu(I)}{\partial I} \right) = \det \left( \frac{\partial^2 H_0(I)}{\partial I^2} \right) \neq 0 \quad (4)$$

the frequency map

$$F : B^n \longrightarrow \mathbb{R}^n; \quad (I) \longrightarrow (\nu) \quad (5)$$

is a diffeomorphism on its image  $\Omega$ , and the tori are as well described by the action variables  $(I) \in B^n$  or in an equivalent manner by the frequency vector  $(\nu) \in \Omega$ .

The system is also called isoenergetically nondegenerate [2] if one of the frequencies ( $\nu_n$  for example) does not vanish and the  $n - 1$  ratios  $(\nu_i/\nu_n)_{i=1, n-1}$  of the remaining frequencies are functionally independent on the energy level  $H_0 = cte$ , which corresponds to the condition

$$\det \begin{pmatrix} \frac{\partial^2 H_0(I)}{\partial I^2} & \frac{\partial H_0(I)}{\partial I} \\ \frac{\partial H_0(I)}{\partial I} & 0 \end{pmatrix} \neq 0. \quad (6)$$

For a nondegenerate system (or for an isoenergetically nondegenerate system), when  $\varepsilon$  is nonzero, the KAM theorem [2] still asserts that for sufficiently small values of  $\varepsilon$ , there exists a Cantor set  $\Omega_\varepsilon$  of values of  $(\nu)$ , satisfying a diophantine condition of the form

$$|(k, \nu)| > \frac{\kappa_\varepsilon}{|k|^m} \quad (7)$$

for which the perturbed system still possess smooth invariant tori with linear flow (denoted the KAM tori). Moreover, according to Pöschel, [26] there exists a diffeomorphism

$$\Psi : \mathbb{T}^n \times \Omega \longrightarrow \mathbb{T}^n \times B^n; \quad (\varphi, \nu) \longmapsto (\theta, I) \quad (8)$$

which is analytical with respect to  $\varphi$  and  $C^\infty$  in  $\nu$  and on  $\mathbb{T}^n \times \Omega_\varepsilon$  transforms the Hamiltonian equations into

$$\dot{\nu}_j = 0, \quad \dot{\varphi}_j = \nu_j . \quad (9)$$

For frequency vectors ( $\nu$ ) belonging to  $\Omega_\varepsilon$ , the solution thus lies on a torus and is given in complex form by its Fourier series

$$z_j(t) = z_{j0} e^{i\nu_j t} + \sum_m a_m^j(\nu) e^{i\langle m, \nu \rangle t} , \quad (10)$$

where  $\langle m, \nu \rangle = m_1 \nu_1 + m_2 \nu_2 + \dots + m_n \nu_n$ , and where the coefficients  $a_m^j(\nu)$  depend smoothly on the frequencies ( $\nu$ ). Let us also notice that due to the analyticity of  $\Psi$ , the series  $\sum_m |m|^p a_m^j(\nu)$  are convergent for all  $p \in \mathbb{N}$ . If we fix all values of  $\theta \in \mathbb{T}^n$ , to some arbitrary value  $\theta = \theta_0$ , we obtain a frequency map on  $B$  defined as

$$F_{\theta_0} : B^n \longrightarrow \Omega; \quad I \longmapsto p_2(\Psi^{-1}(\theta_0, I)) , \quad (11)$$

where  $p_2$  is the projection on  $\Omega$  ( $p_2(\phi, \nu) = \nu$ ). It should be noted that for sufficiently small  $\varepsilon$ , the torsion condition (4) ensure that the frequency map  $F_{\theta_0}$  is a diffeomorphism, and if  $(\theta, I)$  and  $(\theta', I')$  belong to the same KAM torus, we have  $F_\theta(I) = F_{\theta'}(I')$ .

The frequency map analysis will consist in obtaining directly, in a numerical manner, a natural frequency map  $F$ , defined on a whole domain  $B^n$ , which will coincide, up to numerical accuracy, with  $F_{\theta_0}$  (11) on the set of the KAM tori. The frequency map  $F$  is obtained by searching for quasiperiodic approximations of the solutions, over a finite time span, in the form of a finite number of terms

$$z_j(t) = z_{j0} e^{i\nu_j t} + \sum_{k=1}^N a_{m_k}^j e^{i\langle m_k, \nu \rangle t} , \quad (12)$$

where the coefficients  $a_{m_k}^j$  are of decreasing amplitude. Once the quasiperiodic approximation (12) is obtained, the construction of the frequency map can be made and the practical study of the global dynamics of the system (1) will then be possible in a very effective manner by the study of the regularity of this frequency map [4, 13, 14, 16, 17, 18].

Assume that an isoenergetically nondegenerate Hamiltonian system is given in the form (1). The motion takes place in the  $2n - 1$  manifold of energy defined by  $H(I, \theta) = h$ . Usually, one can take a Poincaré surface of section (for example  $\theta_1 = 0$ ) which will restrict the study to a  $2n - 2$  dimension space. Although this is very useful for two degrees of freedom systems, it becomes more difficult to use in higher dimensions. Here we adopt a much more drastic reduction of the problem, by fixing all the initial values of the angles to arbitrary values  $\theta_j(0) = \theta_{j0}$  for all  $j = 1, 2, \dots, n$ .

For any initial values of the  $n - 1$  action-like variables  $(I)_{n-1} = (I_1, I_2, \dots, I_{n-1})$  in a domain  $B^{n-1}$ , and for sufficiently small values of  $\varepsilon$ , as the initial angle variables  $(\theta_0)$  are fixed, and as the system is non-degenerated, the last action  $I_n^*$  is determined by the condition  $H((I)_{n-1}, I_n^*, \theta_0) = h$ . We can then carry out a numerical integration of the differential equations over a finite time  $[\tau, \tau + T]$ , where  $T$  is fixed, and  $\tau$  an arbitrary

value of the time. Then, we perform a quasiperiodic approximation of this numerical solution over the time interval of length  $T$ ,  $[\tau, \tau + T]$ . We thus obtain quasiperiodic approximations of the form (10). Out of these approximations, we just retain the frequency vector  $(\nu_1, \nu_2, \dots, \nu_n)$  and construct the frequency map

$$\begin{aligned} F_T : B^{n-1} \times \mathbb{R} &\longrightarrow \mathbb{R}^{n-1} \\ ((I)_{n-1}, \tau) &\longrightarrow \left( \frac{\nu_1}{\nu_n}, \frac{\nu_2}{\nu_n}, \dots, \frac{\nu_{n-1}}{\nu_n} \right). \end{aligned} \quad (13)$$

Let  $\mathcal{A}$  be the subset of  $B^{n-1}$  of the values of  $(I)_{n-1}$  such that  $((I)_{n-1}, I_n^*, \theta_0)$  belongs to a KAM torus of dimension  $n$ . In this case, we can assume that, up to the numerical accuracy of our numerical procedure, the rotation vector  $(\nu)$  is the true rotation vector of the considered torus. We thus assume that on  $\mathcal{A}$ ,  $F_T$  is a very good approximation of the frequency map  $F_{\theta_0}$  defined in (11) and the restriction of the frequency map  $F_T$  to  $\mathcal{A}$  will have thus the following properties :

- a) If  $(I)_{n-1} \in \mathcal{A}$ , then  $F_T((I)_{n-1}, \cdot)$  is constant on  $\mathbb{R}$
- b) For any given  $\tau$ , the map

$$\begin{aligned} F_T^\tau : \mathcal{A} &\longrightarrow \mathbb{R}^{n-1} \\ (I)_{n-1} &\longrightarrow F_T((I)_{n-1}, \tau) \end{aligned} \quad (14)$$

is regular in some sense, as it coincides on  $\mathcal{A}$  with the restriction to  $\mathcal{A}$  of a smooth diffeomorphism.

The criterion (b) ensures that when the frequency map is not regular, the corresponding KAM tori are destroyed. In the case of a two degrees of freedom Hamiltonian, we can even obtain a more precise criterion. Indeed, in this case, and under some condition of non-degeneracy, the frequency map  $F_T : \mathbb{R} \longrightarrow \mathbb{R}$  should be monotonic. As soon as this is not verified for two values of the action like variables  $I_{10}$  and  $I'_{10}$ , we can conclude to the destruction of invariant KAM tori in all the corresponding interval of frequencies  $[F_T(I_{10}), F_T(I'_{10})]$  [16, 14].

### 3. Numerical analysis of the fundamental frequency (NAFF)

The frequency map analysis relies heavily on the observation that when a quasiperiodic function  $f(t)$  in the complex domain  $\mathbb{C}$  is given numerically, it is possible to recover a quasiperiodic approximation of  $f(t)$  in a very precise way over a finite time span  $[-T, T]$ , several orders of magnitude more precisely than what simple Fourier series will provide. Indeed, when one computes the Fourier series of  $f(t)$  over the finite interval  $[-T, T]$ , one assumes that  $f(t)$  is periodic of period  $2T$ , which is obviously not true. In the following algorithm, we make a different hypothesis, which is dictated by the knowledge of the regular dynamics of our system, and we search for quasiperiodic approximations. In this section, we will describe the numerical algorithm (NAFF), which is effectively used for the determination of these quasiperiodic approximations required by the frequency map analysis [12, 13, 16]. Let

$$f(t) = e^{i\nu_1 t} + \sum_{k \in \mathbb{Z}^n - (1, 0, \dots, 0)} a_k e^{i\langle k, \nu \rangle t}; \quad a_k \in \mathbb{C} \quad (15)$$

be a KAM quasiperiodic solution of an Hamiltonian system in  $B^n \times \mathbb{T}^n$ , where the frequency vector  $(\nu)$  satisfies a Diophantine condition (7). The frequency analysis algorithm NAFF will provide an approximation  $f'(t) = \sum_{k=1}^N a'_k e^{i\omega'_k t}$  of  $f(t)$  from its numerical knowledge over a finite time span  $[-T, T]$ . The frequencies  $\omega'_k$  and complex amplitudes  $a'_k$  are found with an iterative scheme. To determine the first frequency  $\omega'_1$ , one searches for the maximum amplitude of

$$\phi(\sigma) = \langle f(t), e^{i\sigma t} \rangle, \quad (16)$$

where the scalar product  $\langle f(t), g(t) \rangle$  is defined by

$$\langle f(t), g(t) \rangle = \frac{1}{2T} \int_{-T}^T f(t) \bar{g}(t) \chi(t/T) dt, \quad (17)$$

and where  $\chi(t)$  is a weight function, that is, a positive and even function with

$$1/2 \int_{-1}^1 \chi(t) dt = 1. \quad (18)$$

In all our computations, we used the Hanning window filter, that is  $\chi(t) = \chi_1(t) = 1 + \cos(\pi t)$ . Once the first periodic term  $e^{i\omega'_1 t}$  is found, its complex amplitude  $a'_1$  is obtained by orthogonal projection, and the process is started again on the remaining part of the function  $f_1(t) = f(t) - a'_1 e^{i\omega'_1 t}$ . It is also necessary to orthogonalize the set of functions  $(e^{i\omega'_k t})_k$ , when projecting  $f$  iteratively on these  $e^{i\omega'_k t}$ . For a KAM solution, the frequency analysis algorithm allows a very accurate determination of the frequencies over the time span  $[-T, T]$ , several orders of magnitude better than with simple FFTs. This is rigorously established by the general theorem given in the Annex, which can be stated as following for a KAM solution (15) and a weight function of the form

$$\chi_p(t) = \frac{2^p (p!)^2}{(2p)!} (1 + \cos \pi t)^p. \quad (19)$$

**Proposition 1** *For a KAM solution  $f(t)$  of the form (15), and using the weight function  $\chi(t) = \chi_p(t)$ , the application of the frequency analysis algorithm over the time span  $[-T, T]$ , as described above, provides a determination  $\nu_1^T$  of the frequency  $\nu_1$  with a precision  $\nu_1 - \nu_1^T$  having the asymptotic expression for  $T \rightarrow +\infty$*

$$\nu_1 - \nu_1^T = \frac{(-1)^{p+1} \pi^{2p} (p!)^2}{A_p T^{2p+2}} \sum_k \frac{\Re(a_k)}{\Omega_k^{2p+1}} \cos(\Omega_k T) + o\left(\frac{1}{T^{2p+2}}\right), \quad (20)$$

$$\text{with} \quad \Omega_k = \langle k, \nu \rangle - \nu_1; \quad A_p = -\frac{2}{\pi^2} \left( \frac{\pi^2}{6} - \sum_{k=1}^p \frac{1}{k^2} \right). \quad (21)$$

In particular, the use of a Hanning data window ( $p = 1$ ) ensures that for a KAM solution, the accuracy of determining the main frequencies will be proportional to  $1/T^4$ , instead of  $1/T^2$  without the Hanning window ( $p = 0$ ), while for an ordinary FFT method, this accuracy will only be proportional to  $1/T$ . The frequency analysis will then easily allow to recover the frequency vector  $(\nu_1, \nu_2, \dots, \nu_n)$ . It should also be stressed that a lot of understanding can already be gained from the examination of the quasiperiodic approximation of the solutions, expressed as (10) [13, 24]. It is also clear that one can investigate the improvements which could result from using larger values of  $p$  or other weight functions.

#### 4. Destruction of KAM tori in 2-DOF systems

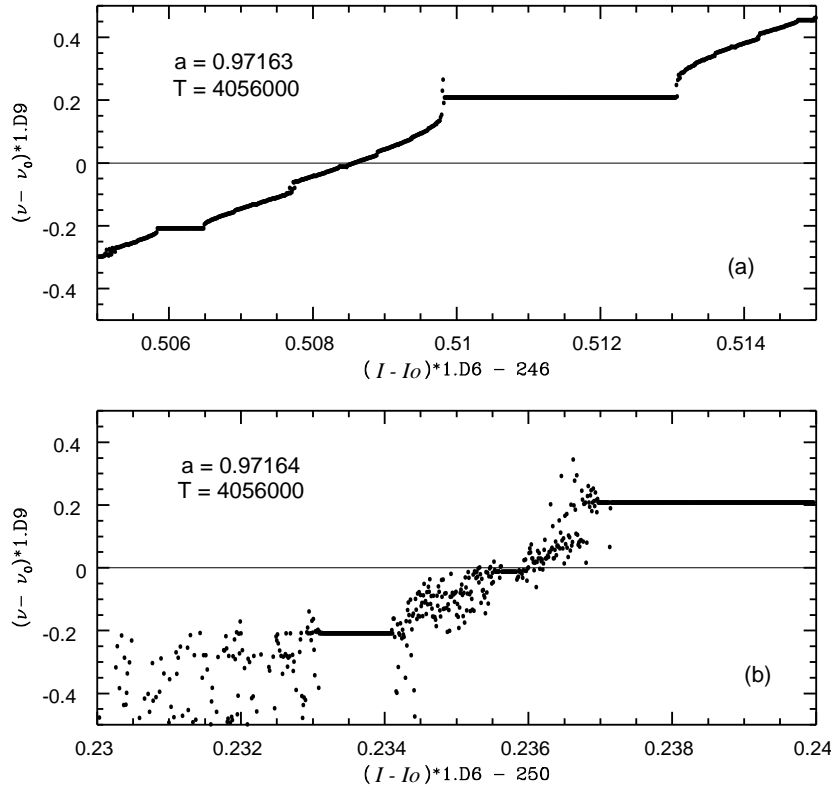
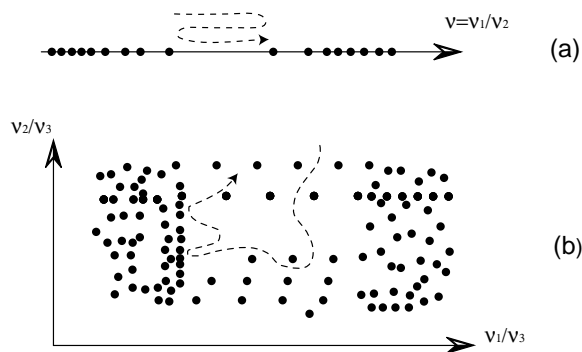


Figure 1. Determination of the critical value of the parameter  $a$  of the standard map ( $I' = I - a \sin \theta$ ,  $\theta' = \theta + I' (2\pi)$ ) for the destruction of the KAM tori of rotation number the golden number  $\nu_0 = (\sqrt{5} - 1)/2$  (horizontal line) by analyzing the regularity of the frequency map over a time span  $T = 4056000$  iterations. It appears clearly that for  $a = 0.97163$ , all motions in the vicinity of the golden tori still behave in a very regular manner, while for  $a = 0.97164$ , the non regularity of the frequency map attests that all rotational KAM tori are destroyed. It should be noted that the frequency and action scales are very small, and the possibility of making such refined studies relies heavily on the very high accuracy of the determination of the frequencies obtained over a limited time span using the NAFF algorithm. The regularity of the plot (a) also suggest that the frequencies are determined with very high precision, even in a very distorted region.

In the case of a 2-DOF (degrees of freedom) nondegenerate Hamiltonian system, or for a two dimensional twist map, the analysis of the frequency map provides a simple criterion for the disappearance of irrational KAM curves [16, 15] which results from Birkhoff's theory for KAM curves (curves of irrational rotation number) (see [8]). Indeed, consider such a map with action like variable  $I$ , and angle variable  $\theta$  with a positive twist condition. For each initial condition  $(I, \theta_0)$  on the vertical line  $\theta = \theta_0$ , we call  $\gamma_I$  the orbit obtained by iterating the mapping and  $\nu_I$  the frequency given by the frequency analysis of this orbit during a given time span. If we make the assumption that (up to numerical accuracy)  $\nu(I) \geq \nu_b$  for any invariant KAM curve  $\gamma_b$  of rotation number  $\nu_b$  which is below  $\gamma_I$ , and that  $\nu(I) \leq \nu_a$  for any KAM curve  $\gamma_a$  of rotation number  $\nu_a$  which is above  $\gamma_I$ , we obtain the following criterion for the non-existence of KAM curves:

*If there exist two values  $I < I'$  on the vertical line  $\theta = \theta_0$  for which  $\nu = \nu(I) > \nu' = \nu(I')$ , then there are no invariant KAM curves of irrational rotation number  $\nu''$  with  $\nu' < \nu'' < \nu$ .*



*Figure 2.* Diffusion of the orbits in the frequency space. The black dots represent KAM tori, and the dotted line, the possible evolution with time of the frequencies for a non-regular orbit. (a) In a 2 degrees of freedom system, the KAM tori divide the frequency space, while in higher dimensions (b), they do not bound the excursion of non-regular orbits, although places containing a large amount of KAM tori can act as practical barriers for the diffusion.

This criterion provides a simple way of knowing whether a KAM curve has disappeared by looking at the graph of the frequency map  $\nu(I)$ , obtained on a given time span  $[0, T]$ . Moreover, according to (14), the nonregularity of the frequency map also shows the destruction of KAM tori on a whole interval of rotation numbers. The figure 1, obtained with  $T = 4056000$ , shows the disappearance of the golden curve for the value  $a = 0.97164$  of the parameter, which is very close to and compatible with the value  $a_c = 0.971635$  derived by Greene [7], while the motion appears very regular for  $a = 0.97163$ . In case of the present twist map, the additional monotonicity criterion provides an easy way to measure the extent of the chaotic region.

## 5. Diffusion in the frequency space

The frequency map (13) can also be used to analyze in a very precise way the diffusion of the orbits in the frequency space [13, 14, 4]. In this case, the initial condition in action ( $I$ ) is also fixed, and the frequency vector ( $\nu$ ) is evaluated over the time interval  $[\tau, \tau + T]$  for different values of  $\tau$ . The time evolution of the numerically determined frequency  $\nu$  can be used to measure the diffusion of the orbit. Indeed, for a KAM tori, the frequency vector is fixed, up to numerical accuracy, while for a non regular orbit, the frequency vector ( $\nu$ ) will evolve with time, revealing the chaotic diffusion of the orbit (figure 2). In a 2-DOF Hamiltonian system, for a fixed level of energy, the frequency space will be a line, so the regular KAM solutions are fixed dots which separates the space, and the chaotic zones are confined by the existing KAM tori. On the contrary, in higher dimension, the KAM tori are still represented as dots in the frequency space, but they do not prevent any longer the chaotic trajectories to wander in the frequency space. Nevertheless, the diffusion is supposed to be extremely small in their vicinity [23, 21]. Thus, for practical view, over finite time, they can be thought to have some width, and regions which are densely filled with such tori will act as effective barriers for limiting the diffusion [14].

## 6. Quasiperiodic perturbation of a 1 degree of freedom system

The non-regular behavior of the frequency map of higher dimensions can be used in general  $n$ -degrees of freedom systems [14, 4], but there is a special case of practical importance

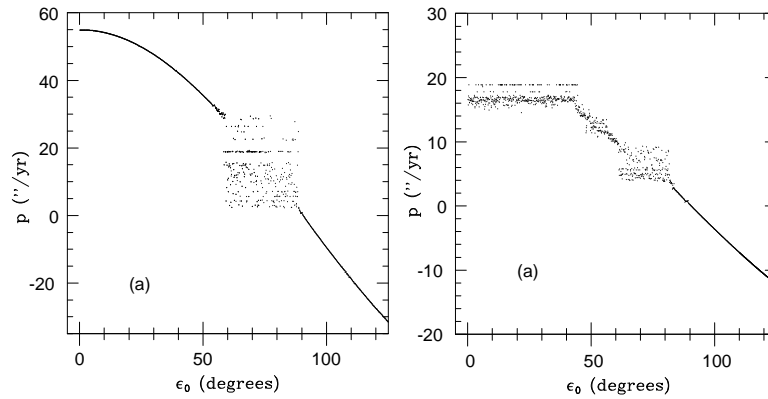


*Figure 3.* Stability of the spin axis of the Earth. The averaged precession frequency  $p$  is measured by means of frequency analysis over a time span  $T$  of about 18 million years, for a wide range of values of the initial obliquity  $\epsilon_0$ . In presence of the Moon (a), there exists a strong chaotic zone, but which is confined in the region from about 60 to 90 degrees. In absence of the Moon (b), the chaotic zone extends from 0 degrees to about 80 degrees, and the tilt of the Earth can suffer extremely large variations [17, 18].

which study is as simple as in the case of two degrees of freedom. This is the case of a  $1+n$  DOF system, i.e. a 1-DOF system perturbed externally by a system with  $n$ -DOF. Here we will even consider only the case of a quasiperiodic forcing, although the general case can also be studied. An interesting example of such a system is given by the precession of the axis of the Earth (or any other planet) which can be describe in a very good approximation by the Hamiltonian

$$H = H_{LS} + H_P \quad \text{with} \quad H_{LS} = \frac{1}{2}\alpha X^2, \quad H_P = \sqrt{1 - X^2} \sum_{k=1}^N \alpha_k \sin(\nu_k t + \psi), \quad (22)$$

where  $X = \cos(\epsilon)$ , and  $\epsilon$  is the obliquity, that is the angle between the spin axis of the Earth and the normal to its orbital plane;  $\psi$  is the precession angle,  $\alpha, \alpha_k$  are real constants, while  $\nu_k$  are combinations of the fundamental secular frequencies of the whole solar system. The first term of the Hamiltonian  $H_{LS}$  describes the action of the Lunar and Solar torques exerted on the equatorial bulge of the Earth, while the complementary part  $H_P$  represents the driving perturbations due to the action of the Solar System [17, 18]. In this case, it is difficult extract interesting information from a surface of section, but the frequency map analysis can be made in a very simple way, exactly as in the case of a 2-DOF system. Indeed, the forcing frequencies are fixed, so, after fixing the starting time  $\tau$  to an arbitrary value ( $\tau = 0$  for example), the frequency map analysis reduces to the study of a simple one dimensional map (fig.3).

$$\begin{aligned} F_T : \mathbb{R} &\longrightarrow \mathbb{R} \\ X &\longrightarrow p, \end{aligned} \quad (23)$$

where  $p$  denotes the precession frequency related to the precession angle  $\psi$ . From this frequency analysis, it thus appear that in the present configuration of the Earth-Moon system, there exists a large chaotic zone for the obliquity of the Earth, from 60 to 90 degrees, while the present tilt of the Earth (at about 23.5 degrees is extremely stable (fig.3a). In absence of the Moon, the precession constant  $\alpha$  is roughly divided by 3, and the chaotic zone increases largely, and extends from 0 degrees to about 80 degrees (fig.3a).

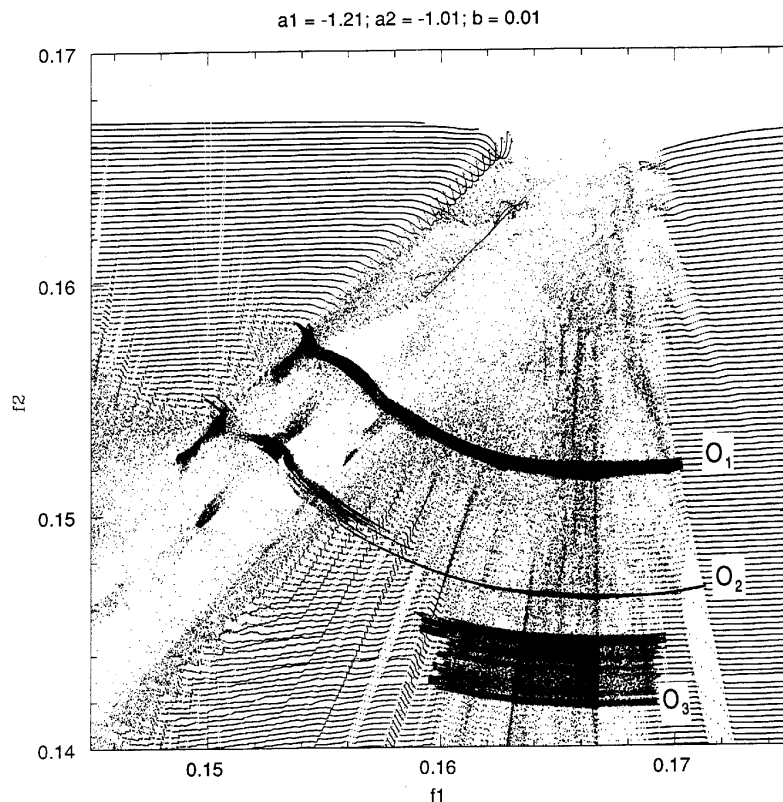


*Figure 4.* Diffusion of orbits in the 4D standard map with  $a_1 = -1.21; a_2 = -1.01; b = 0.01$ . The background is obtained by plotting the image by the frequency map of a mesh of regularly spaced action lines, obtained over 516 iterations. Very high order resonant lines appear as distortion of the frequency map. Three individual orbits ( $O_1, O_2, O_3$ ) are followed over  $10^7$  iterations. This plot reveals in detail the precise path followed by these orbits in the frequency plane. In particular, it appears that large diffusion results from the crossing of many very high order resonance lines. The passage from one resonant line to the next one probably results from some heteroclinic intersection mechanism. It should be also noted that the regular zones acts as practical barriers for the diffusion ([14]).

In such a configuration, the orientation of the Earth would no longer be stable and would suffer extremely large variations. A similar analysis can be conducted with all planets [17, 18].

It should be noted that in the present case of a quasiperiodic external forcing, as with the 2-DOF case, the quasiperiodic solutions will separate the space of motion, and the chaotic zones are strictly limited by the regular orbits. The frequency maps of figures 3 can thus give a very precise account of the possible variations of the obliquity over infinite time. In fact, the real motion of the solar system is not quasi periodic, and a diffusion of the orbital forcing also takes place [13]. This will induce also a possible diffusion for the obliquity, even in the regular regions which appear in figure 3, but this diffusion will be extremely slow.

## 7. Diffusion in 4 dimensional symplectic maps with indefinite torsion

In a previous work [14], the method of frequency map analysis was used to describe the global dynamics and diffusion in the following 4D symplectic map which is the coupling

of two standard maps by a small parameter  $b$  [5]:

$$\begin{cases} I'_1 = I_1 + a_1 \sin(\theta_1 + I_1) + b \sin\left(\frac{1}{2}(\theta_1 + I_1 + \theta_2 + I_2)\right), \\ \theta'_1 = \theta_1 + I_1 \\ I'_2 = I_2 + a_2 \sin(\theta_2 + I_2) + b \sin\left(\frac{1}{2}(\theta_1 + I_1 + \theta_2 + I_2)\right), \\ \theta'_2 = \theta_2 + I_2 \end{cases} \begin{matrix} \text{mod}(2\pi), \\ \\ \text{mod}(2\pi). \end{matrix} \quad (24)$$

For such a dynamical system, the frequency map will have the form

$$\begin{aligned} F_T : \mathbb{R}^2 \times \mathbb{R} &\longrightarrow \mathbb{R}^2 \\ ((I_1, I_2), \tau) &\longrightarrow (\nu_1, \nu_2) \quad , \end{aligned} \quad (25)$$

and for a given value of  $\tau$ , the frequency map is a map of  $\mathbb{R}^2$ , which regularity can be visualized by looking to the image in the frequency plane of a mesh of regularly spaced initial conditions of  $(I_1, I_2)$  (fig.4). This analysis gives a picture of the global dynamics of the mapping, revealing the actual web of resonant and chaotic zones, with their strength. It is also possible to study the diffusion of individual orbits and see how they evolve with time in the frequency space by looking to the restriction of the frequency map for a given initial condition  $(I_1, I_2)$

$$\begin{aligned} \mathbb{R} &\longrightarrow \mathbb{R}^2 \\ \tau &\longrightarrow (\nu_1, \nu_2) \quad . \end{aligned} \quad (26)$$

A striking example of diffusion of orbits is given in figure 4. The background of this figure is obtained by mapping a regular mesh of initial action like variables onto the frequency plane, by means of frequency analysis over only 516 iterations. The 1 : 1 resonance can be clearly seen, as well as the vertical  $f_1 = 1/6$  resonance zone. Many other resonant lines of the form  $\alpha f_1 + \beta f_2 + \gamma = 0$  ( $\alpha, \beta, \gamma \in \mathbb{Z}$ ) resulting from the coupling are clearly visible and appear as distortions of the frequency map. They can be easily identified, and many of them are of very high order, higher than 20 [14]. On the other hand, on both sides of figure 4, exist some very regular regions, where resonant lines do not appear, as they are surely too weak to affect very much the dynamics.

Once this background is obtained, three distinct orbits are followed over an extended time ( $10^7$  iterations). On each interval of 516 iteration, the rotation numbers are determined, so their path can be followed in the frequency plane. It is remarkable that the diffusion is quite rapid, and occurs across the resonance lines. The passage from one resonance line to the next one probably occurring in a quite random way, by some mechanism of heteroclinic intersection. One can also note that the diffusion of these orbits appears to be limited by the regular regions which act as practical fences for the diffusion.

Through the precise analysis of the diffusion of single orbits of figure 4, it thus appears that with the simple analysis of the frequency map over a very limited time (516 iteration) which provides the background of figure 4, one can deduce what can possibly happen over very extended times as  $10^7$  iterations. It is quite clear, for example, that practically no diffusion will occur in the regions which appear as regular for the frequency map. In particular, in these regions, most probably, they will not be any possibility for finding a path which will allow an orbit to escape in a given finite (and reasonable) time. On the contrary, in the non regular zones of the frequency map, fast diffusion can exist, and seems to occur perpendicularly to the resonant lines, which can be of very high order.

It is indeed possible to obtain a heuristic explanation for the striking behavior of the three orbits ( $O_1, O_2, O_3$ ) of figure 4. For this, following [3, 29], it is interesting to consider the mapping (24) as obtained as the return map for the surface of section  $t = 0$  for the Hamiltonian

$$H^+(I_1, I_2, \theta_1, \theta_2, t) = \frac{1}{2}(I_1^2 + I_2^2) + (a_1 \cos \theta_1 + a_2 \cos \theta_2 + 2b \cos((\theta_1 + \theta_2)/2)) \delta_{(1)}(t), \quad (27)$$

where  $\delta_{(1)}(t)$  is the periodic delta-function of period 1. If we average over the periodic terms, we obtain  $(I_1^2 + I_2^2)/2 \approx h$ , where  $h$  is a constant value. We will thus have also for the frequencies  $(\nu_1, \nu_2)$ ,  $(\nu_1^2 + \nu_2^2)/2 \approx h$  which gives trajectories following circles in the frequency plane (figure 5a).

We are here in the presence of a system which is a perturbation of  $H_0^+(I_1, I_2) = (I_1^2 + I_2^2)/2$  which torsion is definite positive. It is thus interesting to investigate the case of non-definite torsion [9]. Such a system can be easily obtained as the return map at  $t = 0$  of the flow of the system of Hamiltonian

$$H^-(I_1, I_2, \theta_1, \theta_2, t) = \frac{1}{2}(I_1^2 - I_2^2) + (a_1 \cos \theta_1 + a_2 \cos \theta_2 + 2b \cos((\theta_1 + \theta_2)/2)) \delta_{(1)}(t) \quad (28)$$

which leads to

$$\begin{cases} I'_1 = I_1 + a_1 \sin(\theta_1 + I_1) + b \sin(\frac{1}{2}(\theta_1 + I_1 + \theta_2 - I_2)), \\ \theta'_1 = \theta_1 + I_1 \\ I'_2 = I_2 + a_2 \sin(\theta_2 - I_2) + b \sin(\frac{1}{2}(\theta_1 + I_1 + \theta_2 - I_2)), \\ \theta'_2 = \theta_2 - I_2 \end{cases} \quad \begin{matrix} \text{mod}(2\pi), \\ \\ \text{mod}(2\pi), \end{matrix} \quad (29)$$

which is the coupling of two standard maps, “turning” in opposite directions. In this case, we will expect to see the frequencies following approximately paths given by  $(\nu_1^2 - \nu_2^2)/2 \approx h$ , which are thus hyperbolas (figure 5b). We also expect to find some isotropic directions where the diffusion will be extremely fast [9, 20].

The frequency map analysis of the system (29) for very similar conditions as in figure 4 is given in figure 6. The results are very striking, As in figure 4, three different trajectories ( $O_1^-, O_2^-, O_3^-$ ) were followed over  $10^7$  iterations. The diffusion trajectories in the frequency space seem to follows in a quite evident way branches of hyperbolas, and the direction  $\nu_1 + \nu_2 = 0$  seems to be actually an isotropic direction with very rapid diffusion. Indeed, the orbit  $O_2^-$  escapes rapidly following this direction, after having spend about 3 million iterations in the vicinity of the resonances  $\nu_1 = 1/6$  and  $\nu_1 + \nu_2 = 0$ . For clearer viewing, the last dots of the escaping orbit are connected.

This numerical analysis thus provides an intuitive understanding of the difference between systems with definite and indefinite torsion, and shows how the latter case should be much more unstable due to the presence of isotropic directions. It should nevertheless be stressed that although the orbits which reach the vicinity of the isotropic directions escape rapidly as  $O_2^-$ , other orbits as  $O_1^-$  and  $O_3^-$  can be chaotic with rapid diffusion (and probably also large Lyapunov exponents), but still practically confined by regular regions in a small area over finite but long time.

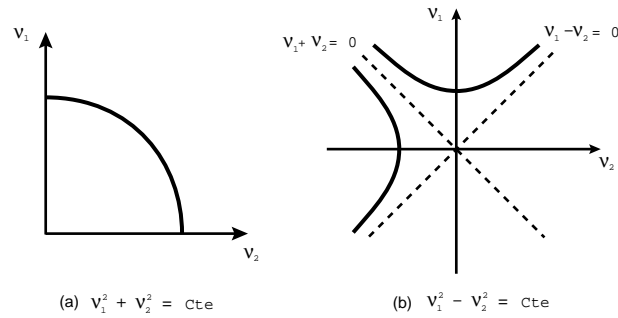


Figure 5.

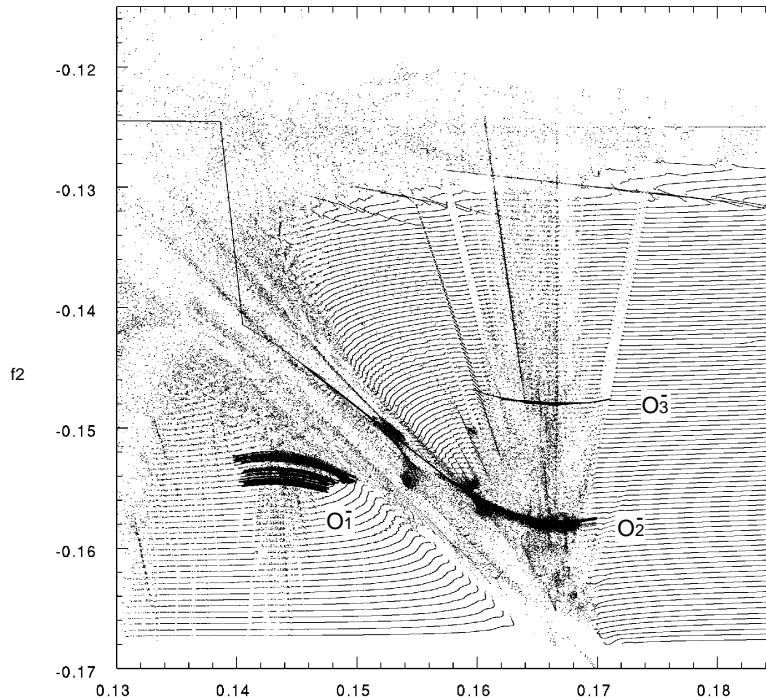


Figure 6. Global dynamics and diffusion for a system with indefinite torsion. The background is obtained by using frequency map with  $T = 516$  iterations, while the three orbits  $O_1^-$ ,  $O_2^-$ ,  $O_3^-$  are followed over  $10^7$  iterations.

It should also be noted that for large perturbations, the torsion signature can change, but its numerical computation by means of frequency map analysis can still be performed, and should thus be a very effective tool for detecting rapid direction of escape and instabilities in systems of practical interest.

### Acknowledgements

It is a pleasure to thank P. Lochak, R. MacKay, and J. Meiss for suggestions on diffusion with indefinite torsion. The evaluation of error in frequency analysis benefited from preliminary studies by F. Joutel and from discussions with A. Albouy, A. Chenciner, D. Sauzin and E. Tabacman. This work was supported by EC contract ERBCHRXCT940460.

## Annex. Convergence of the Frequency Map Analysis

This annex provides a rigorous basis for the frequency map analysis by computing analytic estimates of the precision of the frequencies determined by this method in the case of regular and quasiperiodic solutions.

**Definition 1** A weight function is a positive, even  $C^\infty$  function  $\chi$  on  $[-1, 1]$  such that  $\frac{1}{2} \int_{-1}^1 \chi(t) dt = 1$ . We will call the transform of  $\chi$ , the  $C^\infty$  function on  $\mathbb{R}$ ,  $\varphi_\chi$ , defined as

$$\varphi_\chi(x) = \langle e^{ixt}, 1 \rangle_1^\chi \quad \text{where} \quad \langle f(t), g(t) \rangle_T^\chi = \frac{1}{2T} \int_{-T}^T f(t) \bar{g}(t) \chi(t/T) dt. \quad (30)$$

**Lemma 1** If  $\chi$  is a weight function, we have  $\varphi_\chi(0) = 1$ ;  $\varphi'_\chi(0) = 0$ ;  $\varphi''_\chi(0) < 0$ . For all  $n \in \mathbb{N}$ ,  $|\varphi^{(n)}(x)| < 1$ , and there exists  $M_n > 0$  such that  $|x\varphi^{(n)}(x)| \leq M_n$  on  $\mathbb{R}$ .

*Proof.* As  $\chi(t)$  is even, so is  $\varphi(x)$ , which implies  $\varphi'_\chi(0) = 0$ . We have  $\varphi''_\chi(0) < 0$  as it is the integral of a strictly negative function. We have also  $|\varphi^{(n)}(x)| \leq \frac{1}{2} \int_{-1}^1 |t|^n \chi(t) dt \leq \frac{1}{2} \int_{-1}^1 \chi(t) dt = 1$ . On the other hand, using integration by parts, we obtain  $|x\varphi^{(n)}(x)| \leq (\chi(1) + \chi(-1))/2 + \frac{1}{2} \int_{-1}^1 \chi'(t) dt + n$ . Let us also notice that for all  $n$ ,  $\varphi^{(n)}(x) \in \mathbb{R}$ .

**Definition 2** Let  $\nu = (\nu_1, \nu_2, \dots, \nu_n)$ , and

$$f(t) = e^{i\nu_1 t} + \sum_{k \in \mathbb{Z}^n - (1, 0, \dots, 0)} a_k e^{i\langle k, \nu \rangle t}; \quad a_k \in \mathbb{C} \quad (31)$$

a quasi periodic function on  $\mathbb{R}$ . In the frequency map analysis, the approximation  $\nu_1^T$  of  $\nu_1$  is obtained as the value of  $\sigma$  for which  $\phi(\sigma) = |\langle f(t), e^{i\sigma t} \rangle_T^\chi|$  is maximum in a neighborhood of  $\nu_1$ .

**Theorem 1** Let  $\chi$  be a weight function, and  $\varphi = \varphi_\chi$  its transform with the asymptotic expressions when  $x \rightarrow \infty$

$$\varphi(x) = \frac{g_0(x)}{x^n} + o\left(\frac{1}{x^n}\right), \quad \varphi'(x) = \frac{g_1(x)}{x^n} + o\left(\frac{1}{x^n}\right), \quad \varphi''(x) = \frac{g_2(x)}{x^n} + o\left(\frac{1}{x^n}\right), \quad (32)$$

where  $n \geq 1$ , and where  $g_0(x)$ ,  $g_1(x)$  and  $g_2(x)$  are bounded on  $\mathbb{R}$ . Let  $f(t)$  be a quasi periodic function on the form (31), and for all  $k$ ,  $\Omega_k = \langle k, \nu \rangle - \nu_1$ ; and assume that

$\sum_k \left| \frac{a_k}{\Omega_k^p} \right|$  is convergent for  $p = 0, 1$ , and  $n$ . Then for  $T \rightarrow +\infty$ ,  $\nu_1^T \rightarrow \nu_1$ , and

$$\nu_1 - \nu_1^T = \frac{-1}{\varphi''(0)T^{n+1}} \sum_k \frac{\Re(a_k)}{\Omega_k^n} g_1(\Omega_k T) + o\left(\frac{1}{T^{n+1}}\right). \quad (33)$$

*Proof.* With  $x = (\nu_1 - \sigma)T$ ,  $\nu_1^T$  will be obtained for the maximum value of the modulus of

$$\psi(x) = \varphi(x) + \sum_{k \in \mathbb{Z}^n - (1, 0, \dots, 0)} a_k \varphi(x + \Omega_k T) \quad (34)$$

or, in an equivalent way, the maximum of its square  $\psi(x)\bar{\psi}(x)$ . This maximum thus fulfills the condition  $\psi'(x)\bar{\psi}(x) + \psi(x)\bar{\psi}'(x) = 0$ , that is

$$\begin{aligned} F(x, T) &= \varphi(x)\varphi'(x) + \sum_{k, l} \Re(a_k \bar{a}_l) \varphi(x + \Omega_k T)\varphi'(x + \Omega_l T) \\ &+ \sum_k \Re(a_k) (\varphi(x)\varphi'(x + \Omega_k T) + \varphi'(x)\varphi(x + \Omega_k T)) = 0. \end{aligned} \quad (35)$$

**Lemma 2** Let  $\chi$  be a weight function, and  $\varphi = \varphi_\chi$  its transform. Let us also assume that the series  $\sum_k |a_k|$  and  $\sum_k \left| \frac{a_k}{\Omega_k} \right|$  are convergent with sum  $S_0$  and  $S_1$ . Then for all  $A > 0$ ,

$$\lim_{T \rightarrow +\infty} \sum_k a_k \varphi(x + \Omega_k T) = 0 \quad (36)$$

uniformly with respect to  $x \in [-A, A]$ .

*Proof.* Let  $\mathcal{F}(x, T) = \sum_k a_k \varphi(x + \Omega_k T)$  and  $\varepsilon > 0$ . With a Taylor expansion of  $\varphi$  at order  $n$ , we have

$$\mathcal{F}(x, T) = \sum_{p=0}^n \frac{x^p}{p!} \sum_k a_k \varphi^{(p)}(\Omega_k T) + \frac{x^{n+1}}{(n+1)!} \sum_k a_k \varphi^{(n+1)}(\xi_k) \quad \text{where } \xi_k \in \mathbb{R}. \quad (37)$$

We have from lemma 1

$$\left| \frac{x^{n+1}}{(n+1)!} \sum_k a_k \varphi^{(n+1)}(\xi_k) \right| \leq \frac{A^{n+1}}{(n+1)!} S_0 \quad (38)$$

and this expression can be made arbitrarily small for sufficiently large values of  $n$ . On the other hand, with the notations of lemma 1

$$\left| \sum_k a_k \varphi^{(p)}(\Omega_k T) \right| = \frac{1}{T} \left| \sum_k \frac{a_k}{\Omega_k} (\Omega_k T) \varphi^{(p)}(\Omega_k T) \right| \leq \frac{M_p}{T} S_1. \quad (39)$$

For any  $\varepsilon > 0$ , there exists thus  $n_0 \in \mathbb{N}$  such that for all  $n > n_0$ , and all  $x \in [-A, A]$ ,

$$|\mathcal{F}(x, T)| = \frac{S_1}{T} \sum_{p=0}^n \frac{A^p}{p!} M_p + \varepsilon \quad (40)$$

and for  $T$  sufficiently large, the sum will be arbitrarily small, which ends the demonstration.

**Corollary 1** With the hypothesis of lemma 2, we have

$$\lim_{T \rightarrow +\infty} F(x, T) = \varphi(x) \varphi'(x) \quad (41)$$

uniformly for  $x \in [-A, +A]$ . The function  $F(x, T)$  can thus be continuously extended in a function  $F^*(x, T) : [-A, A] \times ]0, +\infty] \rightarrow \mathbb{R}$ .

We have also for the derivative

$$\begin{aligned} \frac{\partial F(x, T)}{\partial x} &= \varphi(x) \varphi''(x) + \varphi'^2(x) \\ &+ \sum_k \Re(a_k) \{ 2\varphi'(x) \varphi'(x + \Omega_k T) + \varphi(x) \varphi''(x + \Omega_k T) + \varphi''(x) \varphi(x + \Omega_k T) \} \\ &+ \sum_{k,l} \Re(a_k \bar{a}_l) \{ \varphi(x + \Omega_k T) \varphi''(x + \Omega_l T) + \varphi'(x + \Omega_k T) \varphi'(x + \Omega_l T) \}. \end{aligned} \quad (42)$$

With the hypothesis of lemma 2, we will have

$$\lim_{T \rightarrow +\infty} \frac{\partial F(x, T)}{\partial x} = \varphi(x) \varphi''(x) + \varphi'^2(x) \quad (43)$$

uniformly for  $x \in [-A, +A]$ . The extension  $F^*(x, T)$  thus has a continuous first derivative on  $[-A, A] \times ]0, +\infty[$ . From Lemma 1 and (43), we have  $\partial F^*/\partial x(0, +\infty) = \varphi'(0) < 0$ , we can apply the implicit function theorem (see [27], p.176) to  $F^*(x, T)$  at the point  $(0, +\infty)$ . Thus, there exists a neighborhood  $U$  of  $+\infty$ , and a unique continuous map  $\tilde{x}(T) = x$  such that

$$\lim_{T \rightarrow +\infty} \tilde{x}(T) = 0; \quad F(\tilde{x}(T), T) = 0 \quad \text{for all } T \in U. \quad (44)$$

Once the existence of  $\tilde{x}(T)$  verifying (44) is known, we can obtain a generalized equivalent for  $\tilde{x}(T)$  when  $T \rightarrow +\infty$ .

**Lemma 3** *Let  $\varphi(x)$  be a function on  $\mathbb{R}$ , and  $n \in \mathbb{N}, n > 0$ , and assume that for all  $0 \leq p \leq n$  there exists  $M_p > 0$  such that  $|x^p \varphi(x)| \leq M_p$  for all  $x \in \mathbb{R}$ . Then, for all  $A > 0$ , and all  $0 \leq p \leq n$ , there exists  $N_p > 0$  such that*

$$|X^p \varphi(x + X)| \leq N_p \quad \forall (x, X) \in [-A, +A] \times \mathbb{R}. \quad (45)$$

*Proof.* We have  $X^p \varphi(x + X) = (X + x)^p \varphi(x + X) - \sum_{k=0}^{p-1} C_p^k X^k x^{p-k} \varphi(x + X)$  and the proof is obtained by recurrence on  $p$ .

**Lemma 4** *Let  $\varphi(x)$  be a  $C^\infty$  function on  $\mathbb{R}$ , and assume that*

$$\varphi(x) = \frac{g_0(x)}{x^n} + o\left(\frac{1}{x^n}\right), \quad \varphi'(x) = \frac{g_1(x)}{x^n} + o\left(\frac{1}{x^n}\right), \quad (46)$$

where  $g_0(x)$  and  $g_1(x)$  are bounded on  $\mathbb{R}$ , and that the series  $\sum_k \left| \frac{a_k}{\Omega_k^n} \right|$  is convergent. Then for  $T \rightarrow +\infty$ ,

$$\sum_k a_k \varphi(x(T) + \Omega_k T) = \sum_k \frac{a_k}{\Omega_k^n T^n} g_0(\Omega_k T) + o\left(\frac{1}{T^n}\right). \quad (47)$$

*Proof.* Let

$$\mathcal{F}(T) = T^n \left( \sum_k a_k \varphi(x(T) + \Omega_k T) - \sum_k \frac{a_k}{\Omega_k^n T^n} g_0(\Omega_k T) \right) \quad (48)$$

Thus

$$\mathcal{F}(T) = \sum_k \frac{a_k}{\Omega_k^n} \mathcal{F}_k(T) \quad (49)$$

with  $\mathcal{F}_k(T) = (\Omega_k T)^n \varphi(x(T) + \Omega_k T) - g_0(\Omega_k T)$ . From lemma 3,  $|\mathcal{F}_k(T)|$  is bounded, and the series (49) is uniformly convergent with respect to  $T$ . We thus have

$$\lim_{T \rightarrow +\infty} \mathcal{F}(T) = \sum_k \frac{a_k}{\Omega_k^n} \lim_{T \rightarrow +\infty} \mathcal{F}_k(T). \quad (50)$$

But  $\varphi(x(T) + \Omega_k T) - \varphi(\Omega_k T) = x(T) \varphi'(\xi_k(T))$  with  $|\xi_k(T) - \Omega_k T| \leq |x(T)|$ . Thus, as  $x^n \varphi'(x)$  is bounded on  $\mathbb{R}$ , we have for all  $k$

$$\lim_{T \rightarrow +\infty} \mathcal{F}_k(T) = \lim_{T \rightarrow +\infty} x(T) \frac{(\Omega_k T)^n}{\xi_k^n(T)} \xi_k^n(T) \varphi'(\xi_k(T)) + (\Omega_k T)^n \varphi(\Omega_k T) - g_0(\Omega_k T) = 0, \quad (51)$$

which ends the proof of the lemma.

We have also  $\varphi(x) = 1 + o(x)$ , and  $\varphi'(x) = \varphi''(0)x + o(x)$ . Then applying lemma 4 to  $\varphi$  and  $\varphi'$ , and from (Eq. 44), we obtain

$$\varphi''(0)x(T) + o(x(T)) + \sum_k \frac{\Re(a_k)}{\Omega_k^n T^n} g_1(\Omega_k T) + o\left(\frac{1}{T^n}\right) = 0, \quad (52)$$

from which the proof of the theorem ends easily. We can now apply this theorem to specific examples of weight functions. By direct computation, we obtain

**Lemma 5** *Let  $\chi_p(t) = \frac{2^p(p!)^2}{(2p)!} (1 + \cos \pi t)^p$ . Then for all  $p \in \mathbb{N}$ ,  $\chi_p(t)$  is a weight function with associated transform*

$$\varphi_p(x) = \frac{1}{2} \int_{-1}^1 e^{ixt} \chi_p(t) dt = \frac{(-1)^p \pi^{2p} (p!)^2 \sin x}{x(x^2 - \pi^2) \cdots (x^2 - p^2 \pi^2)}. \quad (53)$$

We have also easily the asymptotic expansions for  $x \rightarrow \infty$

$$\varphi_p^{(n)}(x) = \frac{(-1)^p \pi^{2p} (p!)^2 \sin^{(n)} x}{x^{2p+1}} + o\left(\frac{1}{x^{2p+1}}\right), \quad (54)$$

and the expansion at the origin

$$\varphi_p(x) = 1 + \frac{\varphi_p''(0)}{2} x^2 + o(x^2) \quad \text{with} \quad \varphi_p''(0) = -\frac{2}{\pi^2} \left( \frac{\pi^2}{6} - \sum_{k=1}^p \frac{1}{k^2} \right). \quad (55)$$

Thus, if  $f(t)$  is a quasi periodic function of the form (31), for which  $\sum_k \left| \frac{a_k}{\Omega_k^m} \right|$  is convergent for  $m = 0, 1$ , and  $2p + 1$ , then, for  $T \rightarrow +\infty$ ,

$$\nu_1 - \nu_1^T = \frac{(-1)^{p+1} \pi^{2p} (p!)^2}{\varphi_p''(0) T^{2p+2}} \sum_k \frac{\Re(a_k)}{\Omega_k^{2p+1}} \cos(\Omega_k T) + o\left(\frac{1}{T^{2p+2}}\right). \quad (56)$$

**Remark 1.** If  $f(t)$  is a KAM solution, where  $\nu$  fulfills a diophantine condition, the series  $\sum_k \left| \frac{a_k}{\Omega_k^m} \right|$  are convergent for all  $m$ . So using the weight  $\chi_p$ , we can obtain an accuracy for the frequency analysis of order  $1/T^{2p+2}$  on these solutions, which gives in particular  $1/T^4$  when using the Hanning window ( $\chi_1$ ).

**Remark 2.** We can consider the class of weight functions, for which  $\chi^{(n)}(-1) = \chi^{(n)}(1) = 0$  for all  $n$ , as for example  $\chi^*(x) = c \exp(-1/(1-x^2))$ . In this case, we have for all values of  $n, m$ ,  $\lim_{x \rightarrow +\infty} x^n \varphi_{\chi^*}^{(m)}(x) = 0$ . Thus, for a KAM solution, we will have for all  $m$ ,  $\lim_{T \rightarrow +\infty} T^m (\nu_1 - \nu_1^T) = 0$ .

**Remark 3.** The asymptotic convergence of  $(\nu_1 - \nu_1^T)$  when  $T \rightarrow +\infty$  provides a good indication of the possibilities of the method, but in practice, this asymptotic behaviour will be also limited largely by the value of the involved constant, and probably also by numerical accuracy.

**Remark 4.** The theorem is also valid with the same hypothesis for a more general almost-periodic function of the form  $f(t) = e^{i\omega_1 t} + \sum_{k \in \mathbb{Z}} a_k e^{i\omega_k t}$  with  $\Omega_k = \omega_k - \omega_1$ .

## References

1. Arnold V., Proof of Kolmogorov's theorem on the preservation of quasi-periodic motions under small perturbations of the Hamiltonian, *Rus. Math. Surv.* **18**, N6 (1963) 9–36.
2. Arnold V.: Dynamical Systems III *Springer-Verlag, Berlin*, (1988).
3. Chirikov, B.V., A universal instability of many dimensional oscillator systems, *Physics Reports* **52** (1979) 263–379.
4. Dumas, H. S., Laskar, J.: Global Dynamics and Long-Time Stability in Hamiltonian Systems via Numerical Frequency Analysis, *Phys. Rev. Lett.* **70**, (1993), 2975–2979.
5. Froeschlé, C., On the number of isolating integrals in systems with three degrees of freedom, *Astrophys. and Space Sciences* **14** (1971) 110–117.
6. Giorgilli A., Delshams A., Fontich E., Galgani L., Simó C., Effective stability for a Hamiltonian system near an elliptic equilibrium point, with an application to the restricted three body problem, *J. Diff. Equa.* **77** (1989) 167–198.
7. Greene, J.M., A method for determining stochastic transitions, *J. Math. Phys.* **20** (1979) 1183.
8. Herman, M.R., Sur les courbes invariantes par les difféomorphismes de l'anneau. Volume 1, *Astérisque* **103–104** (1983) .
9. Herman, M.R.: Dynamics connected with indefinite normal torsion, *preprint*, (1990).
10. Knezević, Z., and Milani, A.: Asteroid proper elements: the big picture, in Symposium IAU 160, A. Milani, M. Di Martino, A. Cellino, eds, (1994), 31–44, Kluwer, Dordrecht.
11. Kolmogorov, A.N.: 1954, On the conservation of conditionally periodic motions under small perturbation of the Hamiltonian *Dokl. Akad. Nauk. SSSR*, **98**, (1954), 469.
12. Laskar, J., Secular evolution of the solar system over 10 million years, *Astron. Astrophys.* **198** (1988) 341–362.
13. Laskar, J.: The chaotic motion of the solar system. A numerical estimate of the size of the chaotic zones, *Icarus*, **88**, (1990), 266–291.
14. Laskar, J., Frequency analysis for multi-dimensional systems. Global dynamics and diffusion, *Physica D* **67** (1993) 257–281.
15. Laskar, J., Frequency map analysis of an Hamiltonian system, *Workshop on Non-Linear dynamics in Particle accelerators, Arcidosso sept. 1994*, (1995) *AIP Conf. Proc.*, **344**, 130–159.
16. Laskar, J., Froeschlé, C., Celletti, A., The measure of chaos by the numerical analysis of the fundamental frequencies. Application to the standard mapping, *Physica D*, **56**, (1992) 253–269.
17. Laskar, J. Robutel, P.: The chaotic obliquity of the planets, *Nature*, **361**, (1993), 608–612.
18. Laskar, J., Joutel, F., Robutel, P., Stabilization of the Earth's obliquity by the Moon, *Nature* **361** (1993) 615–617.
19. McGill C., Binney, J.: Torus construction in general gravitational potentials, *Mon. Not. R. astr. Soc.*, **244**, (1990) 634–645.
20. morbidelli, A.: Asteroid secular resonant proper elements, *Icarus*, **105**, (1993), 48–66.
21. Morbidelli, A., Giorgilli, A.: Superexponential stability of KAM tori, *J. Stat. Phys.* **78**, (1995) 1607–1617.
22. J.K. Moser, *Nachr. Akad. Wiss. Göttingen, Math. Phys. Kl. II* (1962), 1–20.
23. Nekhoroshev, N.N.: An exponential estimates for the time of stability of nearly integrable Hamiltonian systems, *Russian Math. Surveys*, **32**, (1977), 1–65.
24. Papaphilippou, Y., Laskar, J.: Frequency map analysis and global dynamics in a two degrees of freedom galactic potential, (1996) *Astron. Astrophys.*, (in press).
25. Poincaré, H.: Les Méthodes Nouvelles de la Mécanique Céleste, tomes I-III, *Gauthier Villard, Paris*, (1892-1899), reprinted by Blanchard, 1987.
26. J. Pöschel: Integrability of Hamiltonian systems on Cantor sets, *Comm. Pure Appl. Math.* **25** (1982), 653–695.
27. Schwartz, L.: Analyse, t. II. Calcul différentiel et équations différentielles, *Hermann, Paris*, 1992.
28. R.L. Warnock and R. D. Ruth, Long-term bounds on nonlinear Hamiltonian motion, *Physica D* **56** (1992) 188–215.
29. Wisdom, J., Chaotic behaviour and the origine of the 3/1 Kirkwood gap, *Icarus* **56** (1983) 51–74.



## Table of Contents

<b>J. Laskar</b>	<b>131</b>
<b>1 INTRODUCTION TO FREQUENCY MAP ANALYSIS</b>	<b>131</b>